Applied Catalysis B: Environmental 86 (2009) 182–189

Contents lists available at ScienceDirect

Applied Catalysis B: Environmental

journal homepage: www.elsevier.com/locate/apcatb

Catalytic wet air oxidation of dye pollutants by polyoxomolybdate nanotubes under room condition

Yang Zhang [a], Dongliu Li [a], Yang Chen [a], Xiaohong Wang [a,*], Shengtian Wang [b,**]

[a] Key Lab of Polyoxometalate Science of Ministry of Education, Faculty of Chemistry, Northeast Normal University, Changchun 130024, PR China
[b] Faculty of Chemistry, Northeast Normal University, Changchun 130024, PR China

ARTICLE INFO

Article history:
Received 28 December 2007
Received in revised form 30 July 2008
Accepted 4 August 2008
Available online 22 August 2008

Keywords:
Catalytic wet air oxidation
Safranin-T
Wastewater treatment
Polyoxometalates

ABSTRACT

In order to develop a catalyst with high activity and stability for catalytic wet air oxidation of pollutant dyes at room condition, a new polyoxometalate $Zn_{1.5}PMo_{12}O_{40}$ with nanotube structure was prepared using biological template. The structure and morphology were characterized using infrared (IR) spectra, UV–vis diffuse reflectance spectra (DR-UV–vis), elemental analyses, X-ray powder diffraction (XRD), and transmission electron microscopy (TEM). And the degradation of Safranin-T (ST), a hazardous textile dye, under air at room temperature and atmospheric pressure was studied as a model experiment to evaluate the catalytic activity of this polyoxomolybdate catalyst. The results show that the catalyst has an excellent catalytic activity in treatment of wastewater containing 10 mg/L ST, and 98% of color and 95% of chemical oxygen demand (COD) can be removed within 40 min. And the organic pollutant of ST was totally mineralized to simple inorganic species such as HCO_3^-, Cl^- and NO_3^- during this time (total organic carbon (TOC) decreased 92%). The structure and morphology of the catalyst under different cycling runs show that the catalyst are stable under such operating conditions and the leaching tests show negligible leaching effect owning to the lesser dissolution. So this polyoxomolybdate nanotube is proved to be a heterogeneous catalyst in catalytic wet air oxidation of organic dye.

1. Introduction

Wet air oxidation (WAO) is very useful for treatment a variety refractory pollutants in wastewater, but the high pressure (0.5–20 MPa) and high temperature (175–320 °C) needed for its operation [1–3] which limits the practical application. So it is necessary to study into this process under mild conditions. Catalytic wet air oxidation (CWAO) is recently developed to relax the oxidation condition [4]. Although catalysts can relax the reaction conditions, CWAO still requires a temperature in the range of 80–180 °C and a pressure in the range of 1–5 MPa [2,5,6], which result in higher installation costs and limit its application in industry widely. Catalyst is the key to a CWAO process, seeking an effective catalyst is the challenge for the study. Donlagic and Levec [7] reported that CWA of Orange II with $CuO–ZnO–Al_2O_3$ catalysts at 230 °C and 1 MPa oxygen partial pressure, and found that high total organic carbon (TOC) removals (88%) can be achieved in 1.5 h. Verenich and Laari [8] has used $CuSO_4$ for the WO of concentrated wastewaters and obtained around 80% COD reduction with a retention time of 2 h at 200 °C and 1 MPa oxygen partial pressure. Chang et al. [9] investigated the CeO_2 catalytic degradation of dye. This catalyst demonstrated above 95% COD removal after oxidation for 2 h at 165 °C and 1 MPa oxygen partial pressure. But in recent years, there are only limited number of studies on the CWAO of organic pollutants under room temperature and atmospheric pressure [3]. Liu and Sun [3] reported $Fe_2O_3–CeO_2–TiO_2/Al_2O_3$ can act as catalyst for the wet air oxidation of methyl orange azo dye under room condition, in which 98.09% of color and 96.08% of TOC can be removed in 2.5 h at room temperature and atmospheric pressure.

Heteropolyacids (HPAs) also named polyoxometalates (POMs) are oxo-clusters of early transition metals in the highest oxidation state, namely Mo (VI), W (VI) or V (V), etc., which represent an increasing important class of environmentally friendly catalysts. Because of their formidable structural variety and specific properties including nano-sized dimension, shape, change, density and surface reactivity, POMs catalyze the oxidation of a number of organic substrates in the presence of either molecular oxygen or other donors [10] even under rather mild conditions. Hill [11] suggested that POMs systems might well find application in consumer products of many kinds that catalyze low-temperature

* Corresponding author at: Key Lab of Polyoxometalate Science of Ministry of Education, Faculty of Chemistry, Northeast Normal University, 5268 Renmin Street, Changchun 130024, Jilin Province, PR China. Tel.: +86 431 88930042; fax: +86 431 85099759.
** Corresponding author.
E-mail address: wangxh665@nenu.edu.cn (X. Wang).

0926-3373/$ – see front matter © 2008 Elsevier B.V. All rights reserved.
doi:10.1016/j.apcatb.2008.08.010

dark air-based oxidation, in devices to cleanse/purify environments or decontaminate chemical warfare agents, as photocatalysts for pollutant removal in several riches where TiO_2-based photocatalysts are used commercially now [12], and in other areas. Compared to the quickly development of POMs-based photocatalysts for pollutants removal [13], there are only few reports on POMs applied for wet air oxidation of organic pollutants [14,15]. So seeking available POMs applied for CWAO is still a challenge and has academic and commercial value.

In Arslan-Alaton and Ferry's report [15] Keggin structure $Na_2HPW_{12}O_{40}$ were selected as CWAO catalysts degrading azo dye Acid Orange at temperature (160–290 °C) and at p_{H_2O} 0.6–3.0 MPa, respectively. For the high reaction temperature (T = 290 °C), 92% mineralization was obtained after 100 min. At T = 230 °C, completely color removal was achieved in 40 min, whereas only 5 min at T = 290 °C. Birchmeier et al. [16] employed $Na_5PV_2Mo_{10}O_{40}$ to treat phenol in CWO processing under mild reaction conditions (155 °C and 0.93 MPa of oxygen pressure), and found that high COD removals (76%) can be achieved over 1 h. As we all know, HPAs like 12-molybdophosphoric acid (MPA) is often used for oxidation reactions because of its high oxidative ability.

HPA is soluble in most of the solvents and acts as homogeneous catalyst in many reactions. So some efforts have been made to overcome the homogeneity by impregnating it on solid supports. But the major problem in these supported catalysts is the leaching of the active species. Efforts have been made to solve the leaching and solubility problem by modifying HPAs by converting them into their corresponding salts or exchanging with different metal ions [17,18].

In our paper, we report the 12-molybdophosphoric acid-based catalyst modified with exchanging of zinc ions for wet air oxidation of organic pollutant ST with molecular oxygen and air as oxidant under room temperature and atmosphere pressure. This catalyst $Zn_{1.5}PMo_{12}O_{40}$ was prepared using biological template-cellulose fibers associated with surface sol–gel process. The nanotube structure of $Zn_{1.5}PMo_{12}O_{40}$ was replicated of the fibers templates and the wall of the nanotube was constructed by zinc salts of POMs. This nanotube was different from others that grafting POMs into some supporters, which is self-supported nanostructure fabricating only by POM molecules. The reason why zinc ion was selected as exchanging agent is that Zinc oxides has been proven to be useful for promotion of oxidation catalyst for degradation of dyes. So the combination of zinc and 12-molybdophosphoric anion might create synergistic reaction to catalyze the degradation of organic pollutants under CWAO process at a mild condition such as at room temperature and atmosphere pressure. In addition, the combination leads to heterogeneous catalytic process.

2. Experimental

2.1. Materials

$H_3PMo_{12}O_{40}\cdot 14H_2O$ was prepared according to the literature method [19] and identified by IR spectra and elemental analysis. All other reagents were of AR grade and used without further purification. Deionized and double-distilled water was used throughout this study. For oxidation degradation, 1.0 g stock solution of ST was prepared in double-distilled water and aqueous solution of needed concentrations was prepared from the stock solution.

2.2. Physical measurements

Elemental analyses of $Zn_{1.5}PMo_{12}O_{40}$ were carried out using a Leeman Plasma Spec (I) ICP-ES. IR spectra (4000–500 cm^{-1}) were recorded in KBr discs on a Nicolet Magna 560 IR spectrometer. DR-UV–vis spectra (200–600 nm) were recorded on a Cary 500 UV–vis-NIR spectrophotometer. TEM micrographs were recorded on a Hitachi H-600 transmission electron microscope. XRD patterns of the sample were collected on Japan Rigaku Dmax 2000 X-ray diffractometer with Cu Kα radiation (λ = 0.154178 nm). The TOC was monitored using a Shimadzu TOC-VCPH-TOC analysis system.

2.3. Preparation of catalyst $Zn_{1.5}PMo_{12}O_{40}$ nanotubes

The typical synthesis procedure is given as follows: 0.8 g, 3.6 mmol zinc acetate added into 5 mL ethanol solution. $H_3PMo_{12}O_{40}\cdot 14H_2O$ (5.0 g, 2.4 mmol) was dissolved in 20 mL distilled water to form a clear solution. Six pieces of commercial filter papers were placed in a suction-filtering unit. The zinc acetate solution and POMs solution were added dropwise into the filter funnel alternatively for about 20 times, in which the solutions were slowly filtered through the filter papers. Then the filter papers were thoroughly washed with water and ethanol alternatively in order to remove the POMs complex and zinc acetate which did not attach into the filter paper surface. Then the filter papers were dried with airflow. The as-prepared paper/$ZnPMo_{12}$ was calcinated for 6 h at 280 °C in air (heating rate 1 °C min^{-1}) to remove the filter paper. The black powder which was self-supporting nanotube was obtained with yield of 1.8 g.

In the previous reports [14], the POMs $Zn_{1.5}PW_{12}O_{40}$ with nanotubes structures were synthesized using natural cellulosic substances as template. In this paper, we used $Zn(AC)_2$ and $H_3PMo_{12}O_{40}$ as precursors to fabricate $Zn_{1.5}PMo_{12}O_{40}$ nanotubes. As we all know that polyoxomolybdate exhibits higher oxidative ability than polyoxotungstate does, $H_3PMo_{12}O_{40}$ was selected as oxidative catalyst in air degradation of organic dye due to its higher catalytic activity. The formation procedure of $Zn_{1.5}PMo_{12}O_{40}$ nanotubes can be found as the same way as Ref. [14].

2.4. Procedure of CWAO experiments

The stoichiometry of reaction was determined by allowing 10 mg/L of ST to react with air at room temperature in the presence of the catalyst. A general procedure was carried out as follows: 1.0 g/L of catalyst $Zn_{1.5}PMo_{12}O_{40}$ nanotube was suspended in a fresh aqueous dye solution (C_0 = 10 mg/L, 100 mL) in three-neck glass flask. The air was inputted into the bottom of the suspension with the flowing rate 0.08 m^3/h. At given intervals of illumination, a sample of suspension was taken out by filtration. UV–vis spectroscopy was used in the experiment to monitor the degradation of ST.

ST is selected as the model pollutant because it is a well-known textile colorant, which is harmful to human beings. A favored, promising, cleaner, and greener technology for the removal of this pollutant from water and wastewater has attracted considerable attention. By now, photochemical degradation of the hazardous dye ST using TiO_2 catalyst has been carried out by Gupta group [20]. The chemical structure is as shown in Scheme 1.

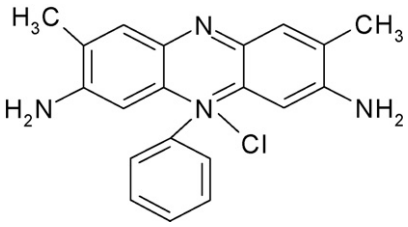

Scheme 1. The structure of ST.

Liquid samples were taken at regular intervals for analysis of absorbance. The visible light absorbance at 524 nm was measured using a UV–vis spectrophotometer

$$\text{Removal}\,(\%) = \frac{A_0 - A}{A_0} \times 100$$

Where A_0 and A are the initial and final absorbance value of dye, respectively.

3. Results and discussion

3.1. Characterization of catalyst $Zn_{1.5}PMo_{12}O_{40}$

From the result of elemental analysis, the contents of the material are Mo, 59.9%; P, 1.6%; Zn, 5.1%, respectively and it can be seen that while the POMs were forming the nanotubes, the ratio of Mo:P:Zn is 12:1:1.5 corresponding to the formula of $Zn_{1.5}PMo_{12}O_{40}$.

The FT-IR spectra of $Zn_{1.5}PMo_{12}O_{40}$ nanotubes were investigated (Fig. 1). The peaks in the IR spectral range 600–1100 cm^{-1} corresponding to $[PMo_{12}O_{40}]^{3-}$ structural vibrations could be distinguished easily at 1060, 955, 870 and 810 cm^{-1}, which were attributed to the asymmetry vibrations P–O_a (internal oxygen connecting P and Mo), Mo–O_d (terminal oxygen bonding to Mo atom), Mo–O_b (edge-sharing oxygen connecting Mo) and Mo–O_c (corner-sharing oxygen connecting Mo_3O_{13} units), respectively [19].

The DR-UV–vis spectrum (Fig. 2) of $Zn_{1.5}PMo_{12}O_{40}$ nanotubes, two characteristic absorbance bands at 237 and 331 nm, corresponding to oxygen to molybdenum charge transfer $O_d \rightarrow Mo$ and $O_b/O_c \rightarrow Mo$, respectively, verifies the existence of PMo_{12} in the nanotubes.

To identify the structure of the $Zn_{1.5}PMo_{12}O_{40}$ nanotubes, XRD spectroscopy was performed and result is given in Fig. 3. All the diffraction peaks could be readily indexed to tetragonal $PMo_{12}O_{40}$ phase (JCPDS No. 75-1588). XRD result also confirms that the heteropolyanion in the as-prepared nanotubes retains its original Keggin-type molecular structure.

The morphology and microstructure of the $Zn_{1.5}PMo_{12}O_{40}$ nanotubes were observed by TEM. The TEM image in Fig. 4 shows that the sample displayed tube-like shapes. The $Zn_{1.5}PMo_{12}O_{40}$ nanotubes with different average diameters from 12 to 20 nm were used in the experiment, respectively. The result showed the average length of the tubes is about 300 nm, and the width of the tubes is about 16 nm, the inner width is about 6 nm.

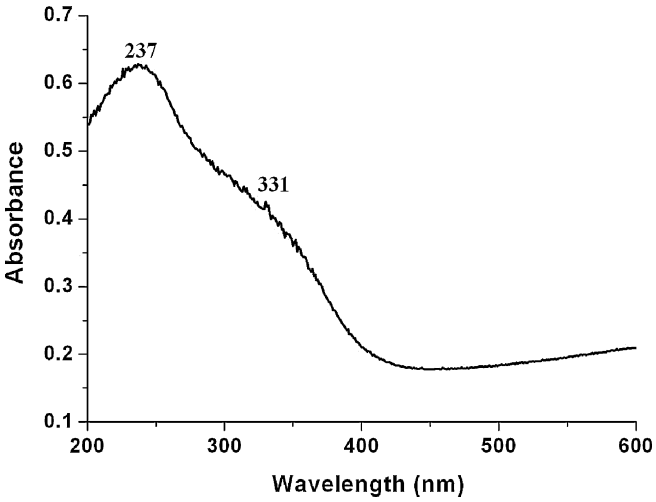

Fig. 2. The UV–vis pattern of the $Zn_{1.5}PMo_{12}O_{40}$ nanotubes.

3.2. Catalytic activity of $Zn_{1.5}PMo_{12}O_{40}$

3.2.1. Determination of the operational window

The investigation into the degradation of 10 mg/L of ST with $Zn_{1.5}PMo_{12}O_{40}$ as catalyst is shown in Fig. 5 under air at room temperature in order to ascertain the usage of $Zn_{1.5}PMo_{12}O_{40}$ on decolorization of ST. Accordingly, the color removal rate is increased significantly by increasing the amount of catalyst. The highest decolorization rate is obtained in the presence of 1.0 g/L $Zn_{1.5}PMo_{12}O_{40}$, and the rate of degradation of ST remains almost constant while increasing the dose of catalyst.

The air flowing rate is an important parameter in CWAO process (Fig. 6). It can be seen that increasing the amount of flowing air, the degradation of ST is increased from 67 to 98% corresponding to the flowing rates 0.03 and 0.08 m^3/h, respectively. When increasing the amount of air, the decolorization of the ST does not increase obviously due to the saturation of air in the liquid phase. From the above experiments, the operational window is C_{cat} = 1.0 g/L and O_2 flowing rate 0.08 m^3/h.

Using oxygen as oxidant in CWAO process, there exists two main stages containing a physical stage and a chemical stage, in

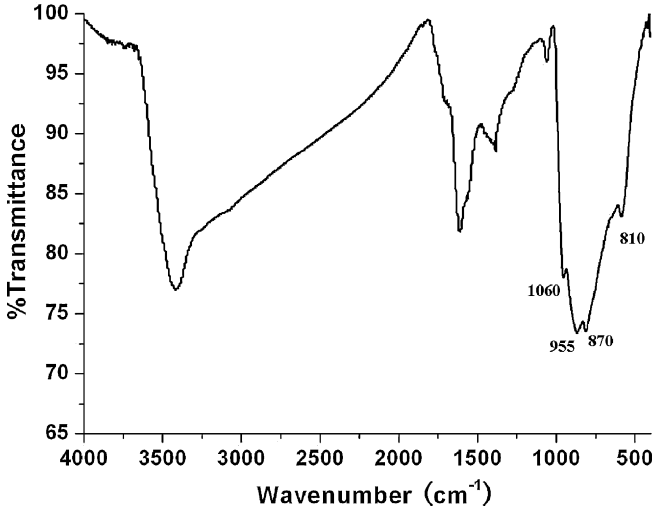

Fig. 1. The FT-IR spectra of $Zn_{1.5}PMo_{12}O_{40}$ nanotubes.

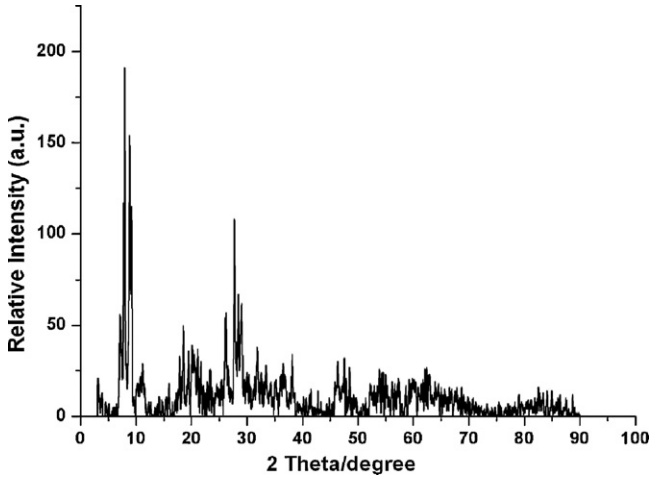

Fig. 3. The XRD pattern of the $Zn_{1.5}PMo_{12}O_{40}$ nanotubes.

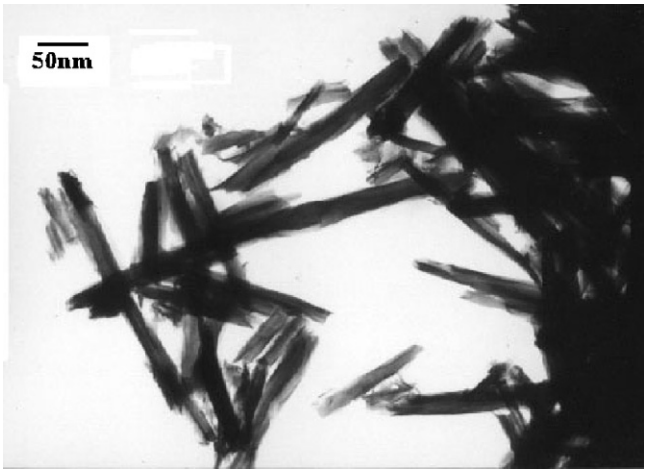

Fig. 4. The typical TEM image of the $Zn_{1.5}PMo_{12}O_{40}$ nanotubes.

which respectively involve transfer of oxygen from the gas phase to the liquid phase, and the reaction between the transferred oxygen (or an active species formed from oxygen) with the organic substrates. In the physical stage, the mass-transfer rate is represented as following [21]:

$$r_m = k_L a(C^*_{O_2} - C_{O_2,L})$$

where r_m is the rate of oxygen mass-transfer, k_L the mass-transfer coefficient, a the gas–liquid interfacial area, $C^*_{O_2}$ the saturation oxygen concentration, and $C_{O_2,L}$ the concentration of oxygen in the liquid. From this equation, it can be seen that the mass-transfer rate is directly proportional to the concentration difference value of $C^*_{O_2} - C_{O_2,L}$. $C^*_{O_2}$ increases as the temperature and oxygen partial pressure each increase. According to the Henry' law, $C^*_{O_2}$ is 44.16 mg/L at our treatment condition, i.e. at 20 °C and 1 atm. As the air flowing rate is 0.08 m^3/h, the $C_{O_2,L}$ is constant. The overall mass-transfer rate r_m is dependent on the interfacial area available between the gas- and liquid-phase. And the increase of gas flow rate can increase interfacial area [22,23] hence increase the rate of oxygen mass-transfer and the decolorization rate. It can be seem from Fig 6, mass-transfer performance is closely related to the airflow rate. In the lower airflow rate, airflow velocity greatly impacts the mass-transfer coefficient, which with the airflow rate

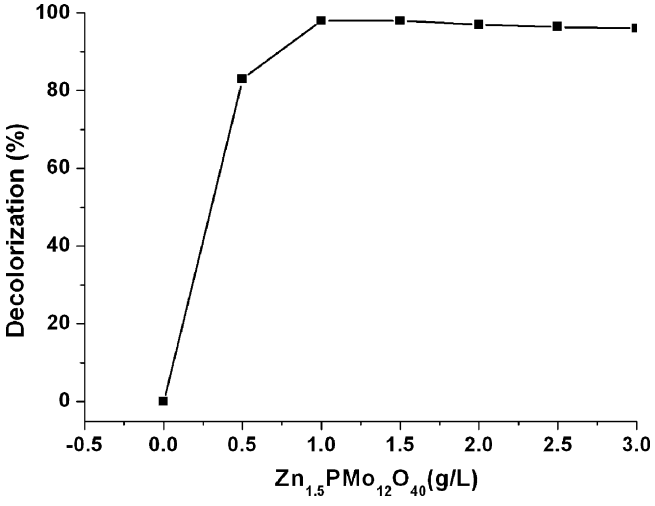

Fig. 5. The effect of $Zn_{1.5}PMo_{12}O_{40}$ concentrations on decolorization of ST in 40 min at room temperature by 100 mL of 10 mg/L ST solution, with the flowing rate 0.08 m^3/h.

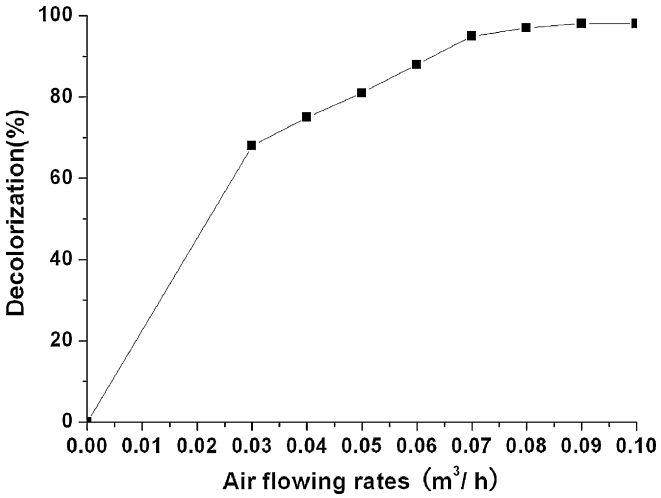

Fig. 6. Degradation of ST under different air flowing rates in 40 min at room temperature by 1.0 g/L catalyst, 100 mL of 10 mg/L ST solution.

increasing, the mass-transfer coefficient increases significantly. In higher airflow rate, airflow rate exhibits less effect on the mass-transfer coefficient. So it can be concluded that at the airflow rate 0.08 m^3/h, the rate of oxygen mass-transfer is constant, in which the decolorization activity comes from the catalytic activity.

3.2.2. Effects of the catalyst

Under above operational window, the investigation into the degradation of 10 mg/L of ST with or without $Zn_{1.5}PMo_{12}O_{40}$ as catalyst is shown in Fig. 7 as a function of time under air at room temperature. Without catalyst $Zn_{1.5}PMo_{12}O_{40}$, but with air flowing only, decolorization efficiency (curve e) is 4.1% in 40 min and in the beginning of 5 min there is no ST degraded. This result shows the oxidation ability of oxygen is limited under room temperature without catalyst. With $Zn(AC)_2$ catalyst and flowing air, decolorization efficiency (curve d) is 6% in 40 min, which shows $Zn(AC)_2$ almost has no catalytic effect. With $Zn_{1.5}PMo_{12}O_{40}$ catalyst and

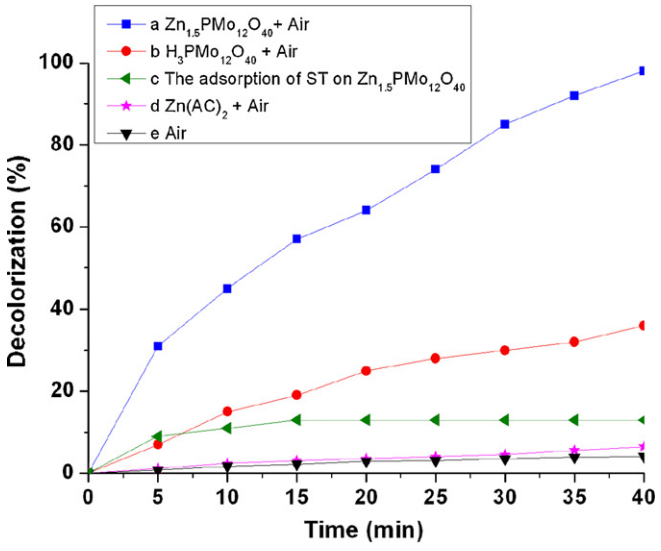

Fig. 7. Decolorization efficiency of ST under different conditions within 40 min at room temperature by 1.0 g/L catalyst, 100 mL of 10 mg/L ST solution, with the flowing rate 0.08 m^3/h. (a) With $Zn_{1.5}PMo_{12}O_{40}$ catalyst and flowing air. (b) With $H_3PMo_{12}O_{40}$ catalyst and flowing air. (c) The adsorption of ST on $Zn_{1.5}PMo_{12}O_{40}$. (d) With $Zn(AC)_2$ catalyst and flowing air. (e) Without catalyst, but with air flowing only.

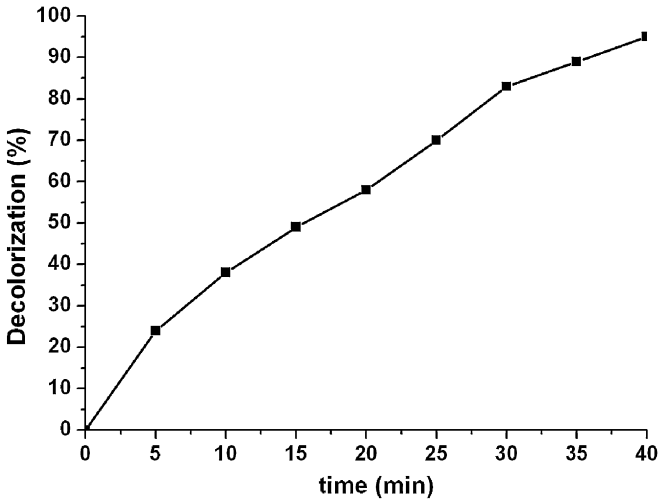

Fig. 8. The COD change of ST under different time at room temperature by 1.0 g/L catalyst, 100 mL of 10 mg/L ST solution, with the flowing rate 0.08 m^3/h.

flowing air, decolorization efficiency (curve a) can be very close to 98% in 40 min, which shows that $Zn_{1.5}PMo_{12}O_{40}$ catalyst exhibits an excellent catalytic activity at such mild condition. Compared with $Zn_{1.5}PMo_{12}O_{40}$ solid catalyst, $H_3PMo_{12}O_{40}$ acts homogeneous catalyst in degradation of ST, the ST decolorization efficiency (curve b) is less than $Zn_{1.5}PMo_{12}O_{40}$ in 40 min, which shows that when forming nanotube structure, the BET surface area is augmented and the catalytic activity is improved.

In order to further evaluate the true activity of catalyst, a series of experiments were carried out to study the adsorption of ST on $Zn_{1.5}PMo_{12}O_{40}$. Fig. 7c illustrates the adsorption isotherm of ST over $Zn_{1.5}PMo_{12}O_{40}$. ST solution (C_0 = 10 mg/L, 100 mL) was treated in the vacuum reactor in the presence of 1.0 g/L $Zn_{1.5}PMo_{12}O_{40}$, which means that there is no oxygen being introduced into the experiment system. It can be seen that in the beginning of the reaction, the concentration of ST decreased 13%, suggesting that slight adsorption of the reactants onto the catalyst occurred. And the concentration of ST remains equilibrium after stirring the suspension after 15 min. So the true decolorization activity comes from the catalyst. The adsorption attributed to the nanotube structure of the $Zn_{1.5}PMo_{12}O_{40}$ nanocomposite, it provides enhanced mass transport for oxygen molecules into and out of the pore structure [24].

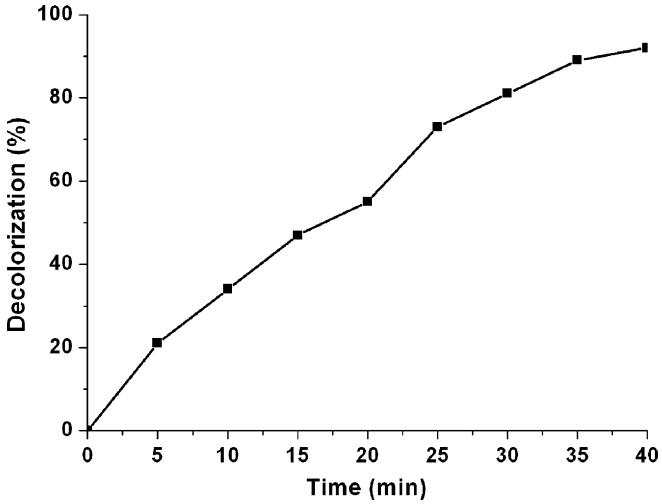

Fig. 9. The TOC change of ST under different time at room temperature by 1.0 g/L catalyst, 100 mL of 10 mg/L ST solution, with the flowing rate 0.08 m^3/h.

3.2.3. Chemical oxygen demand and total organic carbon

Chemical oxygen demand reflects the extent of contamination by the reductive substances in water. It is observed that the ST solutions obtained through CWAO treatment show a significant decrease in COD from 58.3 to 3.1 mg/L (Fig. 8), which the COD removal is about 95%, showing that the high potential of $Zn_{1.5}PMo_{12}O_{40}$ catalyzed CWAO process for the removal of ST from wastewater and the ST is oxidized at the operating conditions. In order to evaluate the catalytic effect on organic dye solution with higher COD value, the decolorization test was carried out using 1.0 g/L $Zn_{1.5}PMo_{12}O_{40}$ catalyst and dye solution with COD value 3 g/L, 10 g/L and 50 g/L. For the dyes with initial COD value 3 g/L and 10 g/L, decolorization can be achieve within 2 h and 5 h, respectively at room condition. For the high initial COD value, i.e. 50 g/L, it needs more amount of catalyst and reaction time in order to the completely decolorization. So we think there are some limitation of the CWAO at room condition comparing to high temperature and press.

To further evaluate the oxidation ability of $Zn_{1.5}PMo_{12}O_{40}$ toward ST, mineralization of ST was studied by monitoring the changes of TOC in reaction systems (Fig. 9). The mineralization ability of as-prepared $Zn_{1.5}PMo_{12}O_{40}$ was strong, and decrease of TOC reached to 92% in 40 min.

It can be seen from Fig. 10 that two major absorbance peaks at 280 and 524 nm in the initial UV–vis spectra of ST, which are due to benzene ring and 2,3-dihydropyrazine ring [25].

As the treatment time increases, these two peaks become weaker and weaker in intensity, and after treatment for 40 min, these two peaks totally disappear, showing that the benzene ring and 2,3-dihydropyrazine ring of ST are destroyed into small species in 40 min.

The typical IR spectra in region 4000–500 cm^{-1} of ST before and after treatment are shown in Fig. 11. The IR spectrum of ST exhibits one aromatic ring C–H stretching vibration peak at 3144 cm^{-1} and three aromatic ring C=C stretching vibration peaks at 1640 and 1493, 1530 cm^{-1}. After treatment ST for about 40 min, these peaks decrease in intensity to disappear, indicating the total destruction of aromatic ring of a ST molecule. In addition, the peaks at 1610 and 1331 cm^{-1} are due to the –N=C– bond and the C–N stretching band of ST molecules. The disappearance of these three peaks associated with destruction of 2,3-dihydropyrazine structure, C–N bond of Ar–NH_2. Moreover, the appearance of new peaks at 1615, 946 and 879 cm^{-1} might be attributed to C–O vibration of HCO_3^- anion. And the new peak at 1045 cm^{-1} due to N–O vibration of

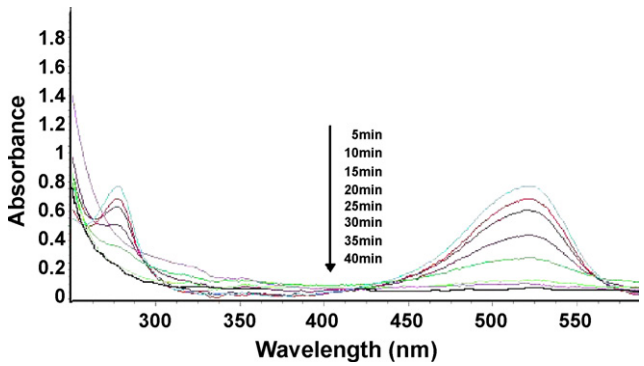

Fig. 10. The UV–vis absorption spectral changes of ST solution in 40 min at room temperature by 1.0 g/L catalyst, 100 mL of 10 mg/L ST solution, with the flowing rate 0.08 m^3/h.

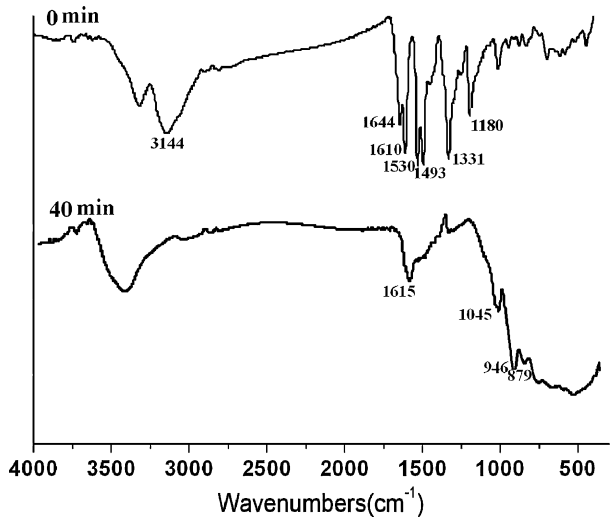

Fig. 11. Degradation of ST under pure oxygen and air flowing in 40 min at room temperature by 1.0 g/L catalyst, 100 mL of 10 mg/L ST solution, with the flowing rate 0.08 m^3/h under air (a) and pure oxygen (b).

NO_3^- anion. There is no Cl^- vibrational peak in the IR spectra because ST is ionic molecule and chlorine exists as Cl^- anion, so $AgNO_3$ is used to detect Cl^- in the final dye, which shows some amount of Cl^- existence in the final dye solution. As results, catalyzed by $Zn_{1.5}PMo_{12}O_{40}$, the organic dye is oxidized by oxygen and subsequently degrades into small inorganic species such as HCO_3^-, NO_3^- and Cl^- anions. The organic dye is totally mineralized as TOC result and this catalyst is available to apply in dye degradation.

3.2.4. Effect of substrate concentration

To study the effect of initial dye concentration on the conversion of the reaction, experiments were carried out with 5, 10, 15 mg/L different concentrations of ST (Fig. 12), while other variables were kept constant. It is found that with the increase in concentration of ST from 5 to 15 mg/L, the rate of degradation decreases, which shows that the color removal depends on its initial concentration. This phenomenon may be due to the fact that with the increase in initial concentration of the dye, which the dose of catalyst is kept constant, more dye molecules are absorbed onto the surface of catalyst $Zn_{1.5}PMo_{12}O_{40}$. Thus, an increase in the number of substrates accommodating in the lattice of catalyst inhibits the action of the catalyst with molecular oxygen, thereby decreases the degradation efficiency.

3.3. Degradation mechanism

Depending on the nature and redox properties of the substrate, electron transfer [26,27], O-transfer [28,29], or radical pathways [30] have been suggested in the oxidation of organic substrates using POMs as catalysts. Generally, organic degradation by wet air oxidation was recognized as a free-radical mechanism and hydroxyl radical is an extremely potential oxidizing agent with a short life which is able to oxidize organic substrates and generate other free radicals [21,31]. With $Zn_{1.5}Mo_{12}O_{40}$ catalyst and bubbled air, decolorization efficiency and decrease of COD can be very close to 98 and 95% in 40 min, respectively, which shows that $Zn_{1.5}PMo_{12}O_{40}$ catalyst exhibits an excellent catalytic activity in such a mild condition and can react with O_2 to generate more $^{\bullet}OH$ radicals to attack dye molecules. The fact that the UV–vis spectrum of the $Zn_{1.5}PMo_{12}{}^{\varepsilon}O_{40}$ species (λ = 237, 331 nm) changes into $Zn_{1.5}PMo_{11}Mo^{\delta}O_{40}$ species (λ = 720 nm) upon mixing with a solution of organic dye and bubbling air confirms this suggestion according to the process outlined in Eq. (1). $^{\bullet}OH$ can be generated by a free radical chain auto oxidation process, which can be described as follows:

$$RH + Zn_{1.5}PMo_{12}{}^{\varepsilon}O_{40} \rightarrow R + H^+ + Zn_{1.5}PMo_{11}Mo^{\delta}O_{40}(\text{catalyticinitiation}) \quad (1)$$

$$R + O_2 \rightarrow RO_2{}^{\bullet}(\text{propagation}) \quad (2)$$

$$RO_2{}^{\bullet} + RH \rightarrow ROOH + R^{\bullet}(\text{propagation}) \quad (3)$$

$$ROOH \rightarrow RO^{\bullet} + {}^{\bullet}OH(\text{autocatalyticdecomposition}) \quad (4)$$

Reaction (2) occurs on the catalyst surface and is a fast reaction, and reactions (3) and (4) are the key steps to produce $^{\bullet}OH$ radical, so increasing the active sites and air amount can prompt reactions (3) and (4) to generate $^{\bullet}OH$, thereby enhance the degradation efficiency of organic pollutants. The tests of air amount (Fig. 6) and the comparison of air and pure oxygen (Fig. 13) confirm this

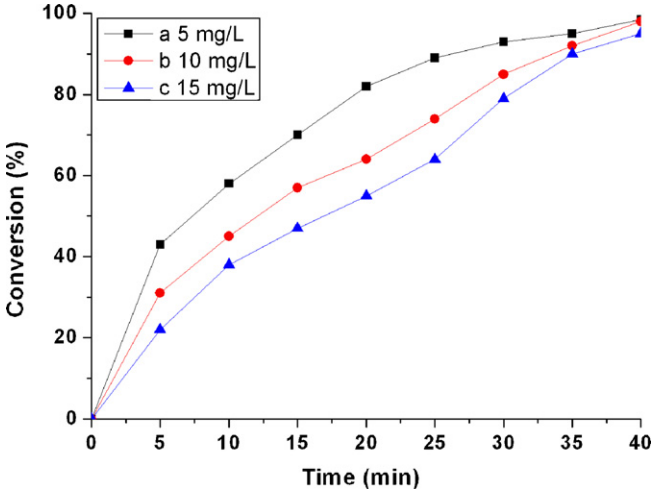

Fig. 12. The effect of substrate concentrations on decolorization of ST in 40 min at room temperature by 1.0 g/L catalyst with the flowing rate 0.08 m^3/h. (a) 5 mg/L ST, (b) 10 mg/L ST and (c) 15 mg/L ST.

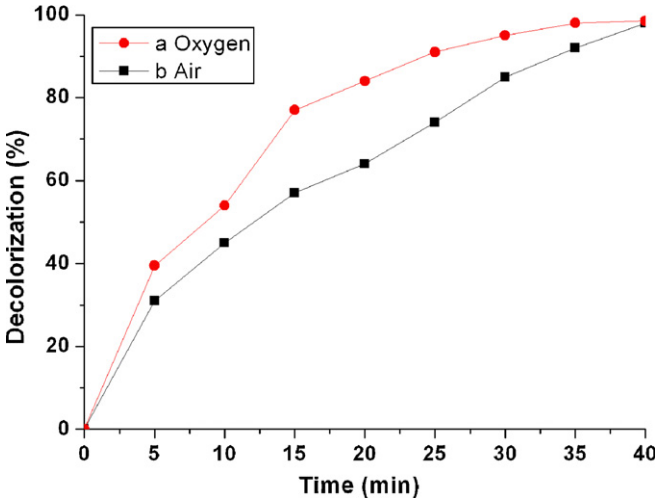

Fig. 13. Changes of ST in FT-IR spectra during degradation.

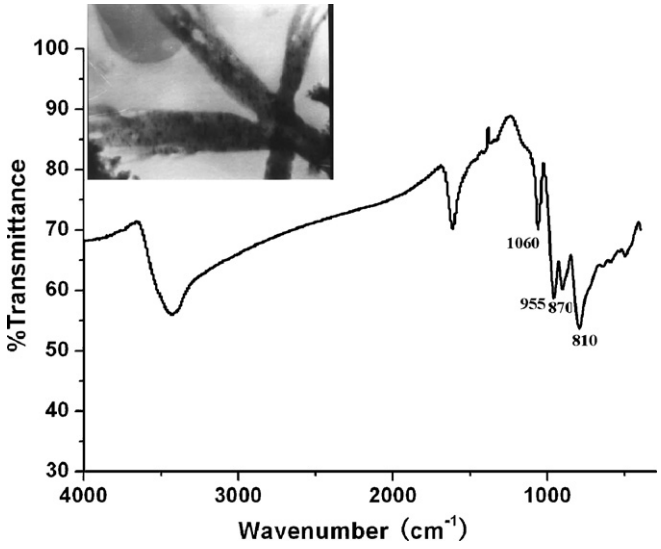

Fig. 14. The FT-IR spectra and TEM (insert) of regenerated $Zn_{1.5}PMo_{12}O_{40}$ nanotubes.

suggestion. From Fig. 11, in comparison of pure oxygen and air, the degradation efficiency under pure oxygen is higher than that under air, which demonstrates the amount of oxygen can effectively influence the degradation efficiency.

POM-catalyzed oxidation undergoes mainly one stage redox cycle. Firstly, an interaction takes place between organic substrate RH and the oxidized form of POMs to generate R radical and the reduced form of POMs. And then •OH can be formed by a free radical chain auto-oxidation process in presence of molecule oxygen so that the organic dyes can be degraded by •OH radical to form inorganic small species such as HCO_3^- and NO_3^- anions. Therefore, the catalytic cycle is completed by re-oxidation of the POM_{red} by molecular oxygen to POM_{ox} form.

3.4. Separation and recovery of the catalyst

After the reactions finished, the suspensions were centrifuged, and the catalysts were decanted to the bottom of the reactor, which is easily to be separated and reused. The amount of Mo determined by ICP-AES in the resulting clear solution was 0.3%, which confirmed the less solubility of the catalyst during the reaction process. The catalysts were thoroughly washed with ethanol and water alternatively in order to remove the ST compound which attached into the catalyst surface then the catalyst is reused in the catalytic experiment. The structure of catalyst did not change after six repeated experiments (Fig. 14). After refreshed, the catalyst still keeps black powder and the morphology does not change (Fig. 14 insert). The catalytic activity of the degradation of ST is maintained efficiently after six repeated experiments with slightly decrease owing to less dissolution (Fig. 15).

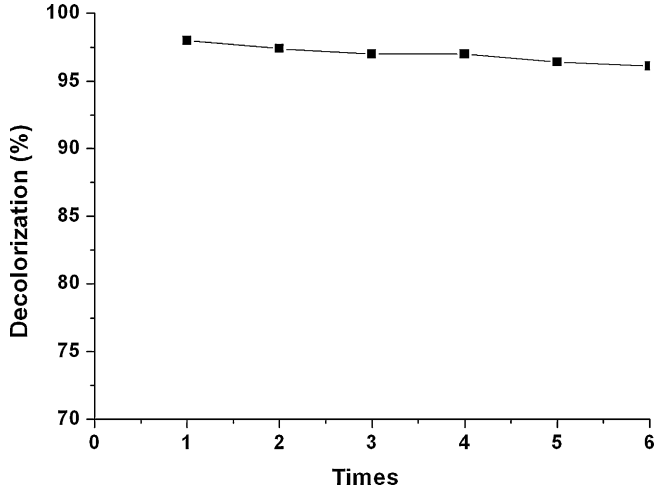

Fig. 15. Cycling runs in the COD removals of ST in the presence of $Zn_{1.5}PMo_{12}O_{40}$ under molecular oxygen in 40 min at room temperature by 1.0 g/L catalyst, 100 mL of 10 mg/L ST solution, with the air flowing rate 0.08 m^3/h.

4. Conclusions

A study was conducted with $Zn_{1.5}PMo_{12}O_{40}$ prepared using native cellulose fiber templates associated with surface sol–gel technique employed as catalyst for CWAO of organic dye ST at room temperature and atmospheric pressure. The synthetic method of catalyst is a unique, convenient, low-cost and green chemical pathway, which is suitable for industrial production. The biological template method is proven to be a flexible way to control the size, structure and higher order organization of inorganic framework. In our prepared procedure of nanotube $Zn_{1.5}PMo_{12}O_{40}$, the nanotube structure was replicated of the fibers templates and the wall of the nanotube was constructed by zinc salts of POMs. This nanotube was different from others that grafting POMs into some supporters, which is self-supported nanostructure fabricated only by POM molecules. And the surface sol–gel approach provides the strong linking between zinc cation and POMs anion leading to formation of stable $Zn_{1.5}PMo_{12}O_{40}$ molecules. In addition, calcination of the precursor under 280 °C leads to form stable and unsoluble $Zn_{1.5}PMo_{12}O_{40}$ salt being used as heterogeneous catalysts. $Zn_{1.5}PMo_{12}O_{40}$ exhibits an excellent catalytic activity in the CWAO process under such a mild room condition and ST molecules are completely mineralized into small inorganic species so that degradation of ST wastewater can be achieved through CWAO treatment for 40 min by adding 1.0 g/L $Zn_{1.5}PMo_{12}O_{40}$ catalyst at an airflow rate of 0.08 m^3/h. The leaching test results indicate less leaching of $Zn_{1.5}PMo_{12}O_{40}$, which can be reused for at least six times. And the IR spectrum and TEM of catalyst after six cycling runs show the stability at six operating condition, which proved that the catalyst overcome the drawback of the heterogeneous catalysts. This catalytic process is a commercial and green chemical pathway which exhibits potential industrial application in dye's degradation. And the studies on the treatment of actual dye wastewater in the same catalytic process are undergoing.

Acknowledgements

Supported by analysis and testing foundation of Northeast Normal University and the major projects of Jilin Provincial Science and Technology Department.

References

[1] Q. Wu, X.J. Hu, P.L. Yue, X.S. Zhao, G.Q. Lu, Appl. Catal. B: Environ. 32 (2001) 151–156.
[2] G. Neri, A. Pistone, C. Milone, S. Galvagno, Appl. Catal. B: Environ. 38 (2002) 321–329.
[3] Y. Liu, D.Z. Sun, Appl. Catal. B: Environ. 72 (2007) 205–211.
[4] D.K. Lee, I.C. Cho, G.S. Lee, S.C. Kim, D.S. Kim, Y.K. Yang, Sep. Purif. Technol. 34 (2004) 43–50.
[5] S.C. Kim, D.K. Lee, Catal. Today 97 (2004) 153–158.
[6] J. Guo, M. Al-Dahhan, Chem. Eng. Sci. 60 (2005) 735–746.
[7] J. Donlagic, J. Levec, Appl. Catal. B: Environ. 17 (1998) L1–L5.
[8] S. Verenich, A. Laari, J. Kallas, Waste Manage. 20 (2000) 287–293.
[9] D.J. Chang, I.P. Chen, M.T. Chen, S.S. Lin, Chemosphere 52 (2003) 943–949.
[10] N. Mizuno, M. Misono, Chem. Rev. 98 (1998) 199–218.

[11] C.L. Hill, Mol. J. Catal. A: Chem. 262 (2007) 2–6.
[12] J.C. Zhao, C.C. Chen, W.H. Ma, Top. Catal. 35 (2005) 269–278.
[13] Y.H. Guo, C. Hu, Mol. J. Catal. A: Chem. 262 (2007) 136–148.
[14] F. Chai, L.J. Wang, L.L. Xu, X.H. Wang, J.G. Huang, Dyes Pigments 76 (2008) 113–117.
[15] I. Arslan-Alaton, J.L. Ferry, Dyes Pigments 54 (2002) 25–36.
[16] M.J. Birchmeier, C.G. Hill Jr., C.J. Houtman, R.H. Atalla, I. Weinstock, Ind. Eng. Chem. Res. 39 (2000) 55–64.
[17] P. Nagaraju, N. Pasha, P.S. Sai Prasad, N. Lingaiah, Green Chem. 9 (2007) 1126–1129.
[18] A. Quintanilla, J.A. Casas, J.A. Zazo, A.F. Mohedano, J.J. Rodriguez, Appl. Catal. B: Environ. 62 (2006) 115–120.
[19] C.R. Deltcheff, M. Fournier, R. Franck, R. Thouvenot, Inorg. Chem. 22 (1983) 207–216.
[20] V.K. Gupta, R. Jain, A. Mittal, M. Mathur, S. Sikarwar, J. Colloid. Interface. Sci. 309 (2007) 464–469.
[21] S.K. Bhargava, J. Tardio, J. Prasad, K. Foger, D.B. Akolekar, S.C. Grocott, Ind. Eng. Chem. Res. 45 (2006) 1221–1258.
[22] F.Z.J. Kastanek, J. Kratochvil, J. Cermak, Chemical Reactors for Gas–Liquid Systems, Ellis Horwood, New York, 1993.
[23] Y.T. Shah, B.G. Kelkar, S.P. Godbole, W.D. Deckwer, AIChE J. 28 (1982) 353–379.
[24] Y. Yang, Q.Y. Wu, Y.H. Guo, C.W. Hu, E.B. Wang, Mol. J. Catal. A: Chem. 225 (2005) 203–212.
[25] F. Wu, N.S. Deng, H.L. Hua, Chemosphere 41 (2000) 1233–1238.
[26] I.A. Weinstock, Chem. Rev. 98 (1998) 113–170.
[27] V.A. Grigoriev, D. Cheng, C.L. Hill, I.A. Weinstock, J. Am. Chem. Soc. 123 (2001) 5292–5307.
[28] A.M. Khenkin, L. Weiner, Y. Wang, R. Neumann, J. Am. Chem. Soc. 123 (2001) 8531–8542.
[29] A.M. Khenkin, R. Neumann, J. Org. Chem. 67 (2002) 7075–7079.
[30] A.I.R.P. Castro, D.V. Evtuguin, A.M.B. Xavier, J. Mol. Catal. B: Enzym. 22 (2003) 13–20.
[31] L.C. Lei, Q.Z. Dai, M.H. Zhou, X.W. Zhang, Chemosphere 68 (2007) 1135–1142.